Theor Chem Account (2008) 119:407–411
DOI 10.1007/s00214-007-0386-3

LETTER

Counter-ion effect in the nucleophilic substitution reactions at silicon: a G2M(+) level theoretical investigation

Yi Ren · Xin Wang · San-Yan Chu · Ning-Bew Wong

Received: 13 July 2007 / Accepted: 13 August 2007 / Published online: 26 September 2007

Abstract Three identity nucleophilic substitution reactions at tetracoordinated silicon atom with inversion and retention pathways: Nu + SiH_3Cl → Nu + SiH_3Cl[Nu = (1)Cl^-, (2) LiCl, and (3) $(LiCl)_2$], are investigated using the G2M(+) theory. Our results show that changing the nucleophile can shift the mechanism (favorable pathway), stepwise from a single-well PES for reaction 1, via a double-well PES for reaction 2, to a triple-well PES for reaction 3, indicating the importance of steric and electronic effects on the S_N2@Si.

Keywords Ion pair · S_N2 reaction · Tetracoordinated silicon · Potential energy surface · Inversion and retention

1 Introduction

Exploring the mechanism and nature of nucleophilic substitution at different atoms has recently become the focus of increasing attention, both experimentally and theoretically. There are indications that the mechanism is different between first- and second-row elements. The well-established S_N2 mechanism with a double-well potential energy surface (PES) is evident for nucleophilic substitution at first-row atoms, e.g., carbon [1,2], nitrogen [3,4], and oxygen [5,6], but an addition-elimination (A–E) pathway usually occurs for substitution at second-row elements, e.g., sulfur [7–10], silicon [11–13], and phosphorus [14]. Recently, some interesting mechanisms were reported for the nucleophilic substitution at these second-row elements. In the studies of gas phase thiolate-disulfide exchange reactions, $R_1S^- + R_2SSR_3 \rightarrow R_1SSR_2 + R_3S^-$ Bachrach et al. [15] found that as R_2 becomes larger, the reaction may not proceed via an A–E pathway and the S_N2 mechanism will operate based on the structural and energetic results. Through systematic and theoretical analyses of elementary S_N2@C, S_N2@Si, and S_N2@P reactions, Bochove et al. [16] showed that increasing the coordination number of the central atom as well as the substituents' steric demand, shifts the S_N2@P mechanism stepwise from a single-well PES [with a central stable intermediate (INT)] that is common for substitution at second-row atoms, via a triple-well PES (with a pre- and post-TS before and after the stable INT), back to the double-well PES that is well known for first-row atoms. These results can also be observed in the follow-up paper about S_N2@Si[$Cl^- + SiR_3Cl(R = H, CH_3, C_2H_5, OCH_3)$] by Bento et al. [18]. Using a combination of temperature-dependent ^{31}P NMR spectroscopy and density functional theory, Fish and co-workers [17] revealed that both S_N2- and A–E-type pathways contributed simultaneously to chloride exchange in the tricyclic phosphorus–carbon cage, showing that the S_N2 mechanism is also possible in the nucleophilic substitution at tri-coordinated phosphorus. In all the above studies, the mechanism of S_N2 reactions at second-row elements usually depends on the structures of substrates, however, it may also be modulated with different nucleophiles.

Electronic supplementary material The online version of this article (doi:10.1007/s00214-007-0386-3) contains supplementary material, which is available to authorized users.

Y. Ren (✉) · X. Wang
Faculty of Chemistry and State Key Laboratory of Biotherapy, Sichuan University, Chengdu 610064, People's Republic of China
e-mail: yiren57@hotmail.com

S.-Y. Chu (✉)
Department of Chemistry, National Tsing Hua University,
Hsinchu 30013, Taiwan, Republic of China
e-mail: sychu@mx.nthu.edu.tw

N.-B. Wong
Department of Biology and Chemistry,
City University of Hong Kong, Kowloon,
Hong Kong, People's Republic of China

It is well known that many important reactions in organic chemistry take place in non-polar or lower polarity solvents and generally involve neutral *contact* ion pairs (called ion pair hereinafter) or ion pair aggregates as nucleophiles instead of free ions [19–21]. The ion pair will have significant ionic character, but the ions are not separated by solvent. The reactivity of an ion pair is expected to be rather different from anionic species [22], but theoretical treatments of ion pair S_N2 reactions are relatively scarce [23–27]. The systematic studies on ion pair S_N2 reactions might begin from the work of Streitwieser et al. They calculated some identity ion pair S_N2@C reactions and got interesting results. These reactions $MX + CH_3X$ (X = F and Cl; M = Li and Na) involve preliminary dipole–dipole pre-complexes, then proceed via cyclic inversion or retention TSs with highly bent X−C−X bonds behaving as assemblies of ions [23]. They also extended the work to the higher alkyls and discussed some steric effects for the ion pair S_N2@C reactions [24]. More recently, Ren et al. made some calculations on the ion pair S_N2@C [26], S_N2@N [27], and S_N2@S [28], and addressed the influence of Li^+ on the geometries and relative energies of the stationary points on the PESs.

With a continued interest in the ion pair S_N2 reactions, here we present how the PES of S_N2@Si changes with different nucleophiles. The ion pair bimolecular nucleophilic substitution reactions at silicon [S_N2(Si)] can be usually applied in the synthesis of compounds containing strong carbon–silicon bond (Eqs. 1, 2). Before the realistic systems are studied, it is helpful and useful to investigate the generality of ion pair S_N2(Si) reactions using the simple models. In this study, the theoretical investigations were carried out on three archetypal symmetric substitution reactions with chlorosilane (SiH_3Cl): free ion reaction (Eq. 3), ion pair reaction of monomeric lithium chloride (Eq. 4) and ion pair reaction of dimeric lithium chloride (Eq. 5), in which the studies about the ion pair S_N2@Si reactions (Eqs. 4, 5), to our best knowledge, were reported for the first time. Two different reaction pathways, inversion and retention, are discussed, respectively.

$$SiCl_4 + LiR \rightarrow RSiCl_3 + LiCl \tag{1}$$

$$Me_3SiCl + KCN \rightarrow Me_3SiCN + KCl \tag{2}$$

$$Cl^- + SiH_3Cl \rightarrow SiH_3Cl + Cl^- \tag{3}$$

$$LiCl + SiH_3Cl \rightarrow SiH_3Cl + LiCl \tag{4}$$

$$(LiCl)_2 + SiH_3Cl \rightarrow SiH_3Cl + (LiCl)_2 \tag{5}$$

The objects of this work are: (1) to explore all possible reaction pathways and obtain the PESs for the three symmetric substitution reactions at silicon; (2) to discuss the factors that may influence the reaction mechanism; and (3) to make comparisons between ion pair S_N2@Si with S_N2@C reactions.

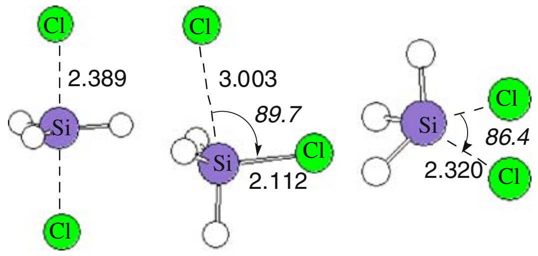

1(inv.INT) **2** (ret.pre-C) **3** (ret.TS)

Fig. 1 B3LYP/6-311+G** optimized stable INT in the inversion pathway, pre-C and TS in the retention pathway involved in the free ion S_N2 reaction (Eq. 3)

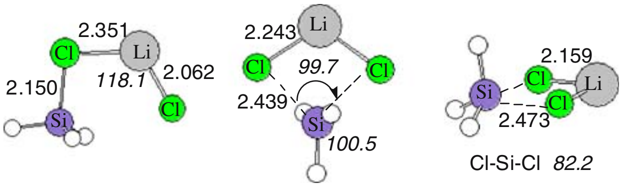

4 (pre-C) **5** (inv.TS) **6** (ret.TS)

Fig. 2 B3LYP/6-311+G** optimized pre-complex, inversion and retention TS involved in the ion pair S_N2 reaction (Eq. 4)

2 Computational methods

A high-level modified Gaussian-2 theory [G2M(+)] theory, which has been successfully applied in the anionic and ion pair S_N2@C reactions [26], showing good agreement with experimental barriers, was used in the present studies. All geometries were optimized by B3LYP/6-311+G** instead of B3LYP/6-311G** in the original G2M method [29]. Electron correlation effect was taken into account by means of CCSD(T) method. Vibrational frequencies were employed to characterize stationary points and the un-scaled zero-point energies were included in comparison to relative energies in kJ/mol. All the TS structures and the reaction pathways were further characterized by intrinsic reaction coordinate (IRC) calculations in the forward and reverse directions. Charge distributions are evaluated by natural population analysis (NPA) [30]. All calculations were performed with Gaussian-98 software package [31]. Throughout this paper, all internuclear distances are in Å and all angles are in degrees.

The main geometries of optimized complexes, intermediates and TSs are shown in Figs. 1, 2 and 3 and the energetics involved in Eqs. 3– 5 are listed in Table 1.

3 Results and discussion

3.1 Free ion reaction

The study of tetra-coordinated silicon compounds began from the pioneer work of Sommer and co-workers [32], and was

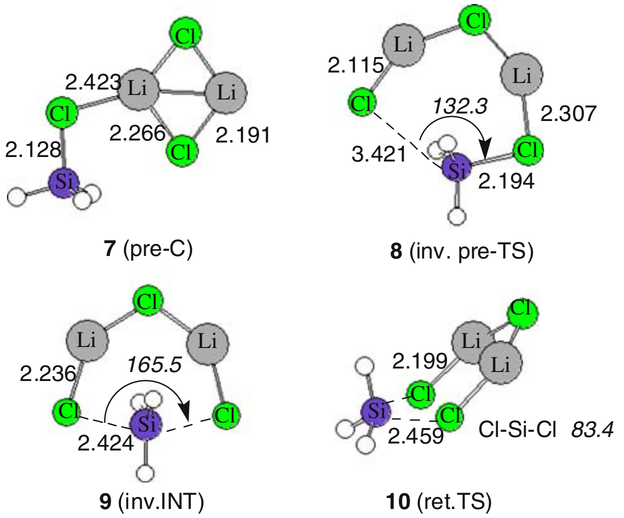

7 (pre-C) **8** (inv. pre-TS)

9 (inv.INT) **10** (ret.TS)

Fig. 3 B3LYP/6-311+G** optimized pre-C, pre-TS, and INT in the inversion pathway, and retention TS involved in the ion pair dimer S_N2 reaction (Eq. 5)

greatly expanded, largely through the efforts of Corriu et al. [33–35]. The accepted inversion pathway for the anionic S_N2@Si reaction (Eq. 3) is that the nucleophile (Cl^-) attacks the central silicon from the backside, giving rise to a symmetric trigonal bipyramidal stable intermediate (INT,**1**) $[Cl\cdots SiH_3\cdots Cl]^-(D_{3h})$, without encountering a first-order saddle point on the PES with entering and leaving Cl^- in axial position, accompanying a single-well PES. The pentavalent siliconate INT **1** is structurally similar to and iso-electronic with the inversion TS in the symmetric S_N2@C reaction, but less Si−Cl bond elongation. The Si−Cl bond order calculated by $\exp[(r\text{-}r^{\neq})/0.6]$ in **1** is 0.60, larger than that for C−Cl bond (0.39) in the inversion TS $[Cl\cdots CH_3\cdots Cl]^{-\neq}$, showing that INT **1** is tighter in structure. Meanwhile the NPA indicates that the silicon atom in **1** bears more positive charge than the carbon atom in $[Cl\cdots CH_3\cdots Cl]^{-\neq}$. The larger size of the central silicon atom with less repulsion between the ligands and the electric factor (stronger attraction between Cl and Si) is responsible for **1** being much lower in energy than free reactants $Cl^- + SiH_3Cl$ by −105.6 kJ/mol at the G2M(+) level, close to the recent best estimated value (−113.4 kJ/mol) at the level of CCSD(T)/aug-cc-pVQZ [36].

The retention process invokes axial attack of Cl^- (to the center of a tetrahedral face containing the leaving Cl^-), resulting in a distorted trigonal bipyramidal ion–dipole pre-complex (pre-C) $[Cl^-\cdots SiH_3Cl$, **2**], with the leaving group in an equatorial position and releasing a complexation energy of −41.2 kJ/mol. The entrance pre-C **2**(Cs) will then pseudorotate to an equivalent exit ion–dipole post-complex (post-C) through the square pyramid TS **3**(Cs) with two Cl^- in *cis*-basal position, bringing the leaving Cl^- to an axial position. Departure of the Cl^- anion from the axial position completes the mechanism. The PES profile for the retention process is double-well with a lower pseudorational barrier of 12.7 kJ/mol relative to **2**. The much lower energy of stable INT **1** than TS **3** suggests that the inversion pathway is more favorable for the ionic S_N2@Si (eq 3).

3.2 Ion pair S_N2 reaction of monomeric lithium chloride and methyl chloride

The PES for the ion pair monomeric S_N2 reaction (Eq. 4) is described by a symmetrical double-well curve. Both the reaction pathways, inversion and retention, involve the initial

Table 1 G2M(+) total energies, E (hartree), energies relative to separated reactants, ΔE (kJ/mol) and the number of imaginary vibrational frequencies (NIMAG) corresponding to the indicated structure (0 = true minimum, 1 = first-order saddle point)

$Cl^- + SiH_3Cl \rightarrow SiH_3Cl + Cl^-$	E	ΔE	NIMAG
$Cl^- + SiH_3Cl$	−1,210.44544	0.0	
$[Cl\cdots SiH_3\cdots Cl]^-$ (INT, **1**)	−1,210.48566	−105.6	0
$Cl^-\cdots SiH_3Cl$ (ret. pre-C, **2**)	−1,210.46115	−41.2	0
ret. TS, **3**	−1,210.45630	−28.5	1 ($268.4i$ cm^{-1})[a]
$LiCl + SiH_3Cl \rightarrow SiH_3Cl + LiCl$			
$LiCl + SiH_3Cl$	−1,217.93002	0.0	
$SiH_3Cl\cdots LiCl$ (pre-C, **4**)	−1,217.94928	−50.5	0
inv. TS, **5**	−1,217.91137	49.0	1 ($331.1i$ cm^{-1})
ret. TS, **6**	−1,217.92692	8.1	1 ($282.7i$ cm^{-1})
$(LiCl)_2 + SiH_3Cl \rightarrow SiH_3Cl + (LiCl)_2$			
$(LiCl)_2 + SiH_3Cl$	−1,685.29744	0.0	
$SiH_3Cl\cdots(LiCl)_2$ (pre-C, **7**)	−1,685.31322	−41.4	0
inv. pre-TS, **8**	−1,685.28630	29.3	1 ($58.5i$ cm^{-1})
inv. INT, **9**	−1,685.29783	−1.0	0
ret.TS, **10**	−1,685.27066	70.3	1 ($275.9i$ cm^{-1})

[a] The number in parentheses corresponds to the sole imaginary frequency for the each TS

formation of an entrance dipole–dipole pre-C. The lithium cation coordinates with the chlorine atom to form a so-called "X-philic" complex $SiH_3Cl \cdots LiCl$ (**4**, C_s), releasing the complexation energy of −50.5 kJ/mol.

In the inversion pathway, this pre-C **4** must overcome a barrier to reach an inversion TS **5**(C_{2V}), in which lithium acts as bridge connecting both halogens, while the SiH_3 group is on a plane perpendicular to the ClSiCl moiety. The inversion TS with inclusion of Li cation shows remarkable deformation from the linear INT geometry **1** and the bridging actions of Li cation causes two chloride anions to be bent towards it with a large decrease of the Cl−Si−Cl angle from 180° to 99.7°. Meanwhile there are significant changes of H−Si−H angles, in which the three H−Si−H angles are 159.0°, 100.5° and 100.5°, respectively, due to the repulsion between negatively charged chlorine and hydrogen atoms. These changes from the favorable Cl−Si−Cl and H−Si−H angles in **1** will increase the repulsion between $Cl^- \cdots Cl^-$ and $H^- \cdots H^-$. The other features in TS **5** are the elongations of the Si−Cl and Li−Cl bonds from 2.150 and 2.062 Å in **4** to 2.243 and 2.439 Å in **5**, respectively. These geometrical deformations will destabilize TS **5** and may be responsible for its higher barrier of 99.5 kJ/mol relative to pre-C **4**, transferring the stable INT structure in the anionic reaction (Eq. 3) into the TS structure in the ion pair monomer reaction (Eq. 4).

For the retention pathway, the coordination of the lithium cation is on the same side of the SiH_3 moiety to both entering and leaving Cl^-, forming retention TS **6**(C_s). In contrast to the inversion TS **5**, the smaller geometry changes relative to pseudoratation TS **3** are likewise observed for TS **6**, in which the already existing acute Cl−C−Cl angles slightly decrease from 86.4° to 82.2° and the Si−Cl bond is increased only by 0.153 Å . Compared with the inversion TS **5**, there is more Si−Cl bond elongation, less elongation of Li−X bond and much smaller Cl−Si−Cl angle changes in the retention TS **6**. Moreover, there are almost no changes of H−Si−H angles from **4** to **6** because the three negatively charged hydrogen atoms are far away from the two chlorine atoms and repulsions between them become much weaker than those in the inversion TS **5**, implying that the retention TS **6** may be more stable than the inversion TS **5** even though the Si−Cl bond is longer and Cl−Si−Cl angle is smaller in TS **6** than that in TS **5**. In fact, the G2M(+) retention barrier relative to free reactants $LiCl + SiH_3Cl$ in Eq. 2 is 8.1 kJ/mol, smaller than that in the inversion pathway by ca. 41 kJ/mol, which suggests that the retention pathway is more favorable for the ion pair monomer S_N2@Si reaction (Eq. 4), different from the corresponding S_N2@C reaction, where the reaction $LiCl + CH_3Cl$ may follow the inversion pathway. This unexpected result probably originates in large part from the lesser deformation energies of SiH_3Cl (180.7 kJ/mol) and LiCl moieties (5.1 kJ/mol) in the retention TS **6** than those (219.4 and 13.4 kJ/mol) in the inversion TS **5**.

3.3 Ion pair S_N2 reaction of dimeric lithium chloride and methyl chloride

When ion pair dimeric aggregates [$(LiCl)_2$, D_{2h}] act as nucleophile, the PES for the inversion pathway of Eq. 5 is demarked by five critical points, corresponding to a pre-C (**7**, Cs), a pre-TS (**8**, Cs), an INT (**9**, C_{2V}), a post-TS (**8**), and a post-C (**7**), constructing a triple-well PES, which indicates that the reaction $(LiCl)_2 + SiH_3Cl$ will follow an A–E mechanism, different from the double-well PES in the corresponding reaction of $(LiCl)_2 + CH_3Cl$ with a central TS [23]. In forming the pre-C **7**, the lithium atom interacts with the chlorine atom, in a similar fashion to the pre-C **4** in Eq. 2. The reaction progresses by having one chlorine atom swing down and moving toward the silicon from backside, forming the pre-TS**8**. Continuing on, one chlorine atom attacks toward silicon and the other chloride atom is away from the silicon simultaneously, reaching the stable INT **9**. The INT **9** in the inversion pathway possesses two equal long Si−Cl distances (2.424 Å) and the Cl−Si−Cl angle is nearly linear (165.5°), which is much larger than that (99.7°) in the ion pair monomer inversion TS **5**. Obviously, incorporation of one more LiCl moiety leads to a significant relief of strain from the distortion of the preferred linear S_N2 attack. This is further confirmed by the population analysis of the INT **2** and **9**. NPA charges on the SiH_3 moiety and attacking or leaving Cl atom change only from 0.384 and −0.692 in **2** to 0.430 and −0.669 in **9**. This result indicates that the dimeric aggregates INT may be comparable to the free ionic INT. The relative energies of the critical points along reaction 3 show that pre-C**7** lies 41.4 kJ/mol below the reactants. The barrier for pre-TS **8** relative to pre-C **7** is 70.7 kJ/mol, while the inversion INT **9** lies 1.0 kJ/mol below the free reactants or 30.3 kJ/mol below the inversion TS **8**.

For the retention pathway involving the ion pair dimer, after forming pre-C **7**, one chlorine atom attacks the central silicon from the front side and the other chlorine is away from the silicon atom, simultaneously, leading to the retention TS **10** (C_s) with a higher reaction barrier of 111.7 kJ/mol relative to pre-C **7**. Comparison with reaction 2 shows that there are geometric similarities for the retention TS **6** and **10**, in which Cl−Si−Cl angles and Si−Cl bonds are almost the same, indicating there is no relief of strain from the incorporation of the second LiCl moiety in the retention pathway of Eq. 3. The larger energy difference (71.3 kJ/mol) between stable INT **9** and TS **10** [also close to the energy difference (77.1 kJ/mol) between stable INT **1** and TS **3**] suggests that the retention pathway can be ignored in the ion pair dimeric aggregates S_N2@Si reaction.

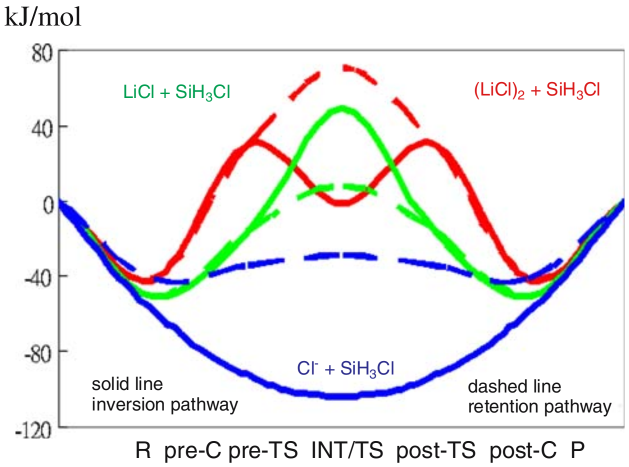

Fig. 4 PES profiles for three S_N2@Si reactions (Eqs. 3–5)

4 Conclusion

In summary, the ion pair monomer nucleophilic substitution at silicon (Eq. 4) follows a classic S_N2 mechanism with a double-well PES due to the strain and stronger repulsions in the four-member ring TSs **5** and **6**, in contrast to the A–E mechanism occurring in the anionic substitution (Eq. 3) with a single-well PES. The unexpected favorable retention pathway for Eq. 4 can be attributed to the smaller deformation energies of SiH_3Cl and LiCl moieties in the retention TS **6**. The incorporation of one more LiCl moiety will significantly reduce the strain and repulsion between negatively charged hydrogen atoms that exist in the ion pair monomer TS **5**, leading to the A–E mechanism with a triple-well PES constructed by the pre-TS and post-TS **8** and the central stable INT **9** in the ion pair dimeric aggregates S_N2@Si reaction (Eq. 5). All the PES profiles are summarized in Fig. 4. These interesting results indicate that the mechanism of S_N2@Si may be modulated with different nucleophiles because the active reagents are often present as monomeric ion pairs or their aggregates when the reaction takes place in non-polar or lower polarity solvents.

Acknowledgments This work is supported by the Ministry of Education (contract 95-2113-M-007-034-MY2) of Taiwan.

References

1. Shaik SS, Schlegel HB, Wolfe S (1992) Theoretical aspects of physical organic chemistry. The S_N2 mechanism. Wiley, New York
2. Laerdahl JK, Uggerud E (2002) Int J Mass Spectrom 214:277
3. Bühl M, Schaefer HF III (1993) J Am Chem Soc 115:9143
4. Glukhovtsev MN, Pross A, Radom L (1995) J Am Chem Soc 117:9012
5. Bachrach SM (1990) J Org Chem 55:1016
6. Ren Y, Wolk JL, Hoz S (2002) Int J Mass Spectrom 220:221
7. Ciuffarin E, Griselli F (1970) J Am Chem Soc 92:6015
8. Ciuffarin E, Guaraldi G (1970) J Org Chem 35:2006
9. Bachrach SM, Gailbreath BD (2001) J Org Chem 66:2005
10. Bachrach SM, Chamberlin AC (2003) J Org Chem 68:4743
11. Damrauer R, DePuy CH, Bierbaum VM (1982) Organometallics 1:1553
12. Davis LP, Burggraf LW, Gordon MS, Baldridge KK (1985) J Am Chem Soc 107:4415
13. Holmes RR (1990) Chem Rev 90:17
14. Søling TI, Pross A, Radom L (2001) Int J Mass Spectrom 210(211):1
15. Bachrach SM, Mulhearn DC (1996) J Phys Chem 100:3535
16. Van Bochove MA, Swart M, Bickelhaupt FM (2006) J Am Chem Soc 128:10738
17. Bento AP, Bickelhaupt FM (2007) J Org Chem 72:2201
18. Fish C, Green M, Kilby RJ, Lynam JM, McGrady JE, Pantazis DA, Russell CA, Whitwood AC, Willans CE (2006) Angew Chem Int Ed 45:3628
19. Winstein S, Savedoff LG, Smith SG, Stevens IDR, Gall JS (1960) Tetrahedron Lett 1:24
20. Streitwieser A, Juaristi E, Kim YJ, Pugh J (2000) Org Lett 2:3739
21. Streitwieser A (2006) J Mol Model 12:673
22. Lai ZG, Westaway KC (1989) Can J Chem 67:21
23. Harder S, Streitwieser A, Petty JT, Schleyer PVR (1995) J Am Chem Soc 117:3253
24. Streitwieser A, Choy GSC, Abu-Hasanayn F (1997) J Am Chem Soc 119:5013
25. Leung SSW, Streitwieser A (1998) J Comput Chem 19:1325
26. Ren Y, Chu SY (2004) J Comput Chem 25:461
27. Ren Y, Chu SY (2004) J Phys Chem A 108:7079
28. Ren Y, Gai JG, Xiong Y, Lee KH, Chu SY (2007) J Phys Chem A 111:6615
29. Mebel AM, Morokuma K, Lin MC (1995) J Chem Phys 103:7414
30. Reed AE, Curtiss LA, Weinhold F (1988) Chem Rev 88:899
31. Frisch MJ et al (1998) Gaussian 98, Revision A.9, Gaussian, Pittsburgh
32. Sommer LH (1973) Intra-Sci Chem Rep 7:1
33. Corriu RJP, Dutheil JP, Lanneau GF (1984) J Am Chem Soc 106:1060
34. Corriu RJP, Dutheil JP, Lanneau GF, Ould-Kada S (1979) Tetrahedron 35:2889
35. Corriu RJP, Lanneau G F, Leclercq D (1983) Phosphorus Sulfur Silicon Relat Elem 18:197
36. Bento AP, Sola M, Bickelhaupt FM (2005) J Comput Chem 26:1497